

## Magnetoresistance Study on $\text{TPP}[M(\text{Pc})(\text{CN})_2]_2$ ( $M=\text{Fe}, \text{Co}, \text{Fe}_{0.30}\text{Co}_{0.70}$ ) Salts

H. Tajima,<sup>\*,1</sup> N. Hanasaki,<sup>\*</sup> M. Matsuda,<sup>\*</sup> F. Sakai,<sup>\*</sup> T. Naito,<sup>†</sup> and T. Inabe<sup>†</sup>

<sup>\*</sup>Institute for Solid State Physics, The University of Tokyo, Kashiwa 277-8581, Japan; and <sup>†</sup>Division of Chemistry, Graduate School of Science, Hokkaido University, Sapporo 060-0810, Japan

Received January 8, 2002; accepted April 25, 2002

The magnetoresistance study on  $\text{TPP}[M(\text{Pc})(\text{CN})_2]_2$  ( $M=\text{Fe}, \text{Co}, \text{Fe}_{0.30}\text{Co}_{0.70}$ ) salts is reported. These three salts have similar columnar structures, nevertheless exhibit different electrical behaviors.  $\text{TPP}[\text{Fe}(\text{Pc})(\text{CN})_2]_2$  exhibits anisotropic giant negative magnetoresistance, while  $\text{TPP}[\text{Co}(\text{Pc})(\text{CN})_2]_2$  exhibits large positive magnetoresistance. The alloyed compound,  $\text{TPP}[\text{Fe}_{0.30}\text{Co}_{0.70}(\text{Pc})(\text{CN})_2]_2$ , also exhibits anisotropic negative magnetoresistance, although the decrease in the resistivity under the magnetic field is less than that of  $\text{TPP}[\text{Fe}(\text{Pc})(\text{CN})_2]_2$ . The  $g$ -tensor anisotropy in the  $[\text{Fe}(\text{Pc})(\text{CN})_2]^-$  unit qualitatively explains the field-orientation dependence of the negative magnetoresistance. Magnetic fluctuation associated with a weak-ferromagnetic transition is suggested as a possible origin of the giant negative magnetoresistance. © 2002 Elsevier Science (USA)

**Key Words:** negative magnetoresistance; phthalocyanine; molecular conductors;  $\pi$ - $d$  interaction; organic conductors; charge-transfer complexes.

### INTRODUCTION

A search for a new function based on the interplay between conduction electrons and local magnetic moments is a current topic in the field of molecular conductors. Most research work concerns charge-transfer complexes composed of molecular donors affording  $\pi$ -conduction electrons and inorganic anions having local magnetic moments. A typical example of such compounds is  $\lambda$ -( $\text{BETS}$ )<sub>2</sub> $\text{FeCl}_4$ , where the successive insulator-metal-superconductor transition driven by the magnetic field is observed at an extremely low temperature (1). The key to synthesize such compounds is the strength of the  $\pi$ - $d$  interaction (the interaction between  $\pi$ -conduction electrons and local magnetic moments). In the case of the charge-

transfer complexes above mentioned, however, this strength is determined by the crystal structure whose design is still beyond control. One of the ways to solve this problem is to synthesize charge-transfer complexes by using the molecules, where the strong  $\pi$ - $d$  interaction is self-contained. In this context, the most promising system is the charge-transfer salts containing metal phthalocyanine,  $(\text{MPc})_x\text{Y}_y$  ( $M$ =metal;  $\text{Pc}$ =phthalocyanine;  $Y$ =counter anion) (2–4). In this system, the conduction band is formed from the  $A_{1u}\pi$ -orbital derived from the  $\text{Pc}$ -ring. This  $A_{1u}\pi$ -orbital is orthogonal to the  $d$ -orbitals of the metal cation at least in a molecule. Therefore, the  $d$ -orbitals are independent from the  $A_{1u}\pi$ -orbital and are potential sources of the local magnetic moments.

Up to now, however, there are few reports for the magnetoresistance studies on  $(\text{MPc})_x\text{Y}_y$  salts (5). The field-orientation dependence of the magnetoresistance has not been reported. This is probably due to the poor quality of single crystals of  $(\text{MPc})_x\text{Y}_y$  salts. Recently, a few of the authors have synthesized new types of phthalocyanine conductors based on the axial-substituted phthalocyanine unit,  $[M(\text{Pc})(\text{CN})_2]^-$  ( $M=\text{Co}, \text{Fe}$ ; see Fig. 1a). Because of the high solubility due to the axial ligands, electrical crystallization is favored, and they succeeded in synthesizing several kinds of conducting crystals with enough quality for transport measurements (6–9). In this paper, we report the magnetoresistance measurements for  $\text{TPP}[M(\text{Pc})(\text{CN})_2]_2$  ( $M=\text{Fe}, \text{Co}, \text{Fe}_{0.30}\text{Co}_{0.70}$ ), where  $\text{TPP}$  denotes the tetraphenylphosphonium cation.

Here, we briefly mention the electronic structure of the  $[M(\text{Pc})(\text{CN})_2]^-$  unit. The electronic structure of this molecular unit can be understood in analogy with that of the  $(\text{MPc})$  molecule. The  $d$ -electrons of  $M^{\text{III}}$  ( $M=\text{Co}, \text{Fe}$ ) in  $[M(\text{Pc})(\text{CN})_2]^-$  are in a low-spin state. According to the Huckel MO calculation, the HOMO of  $[M(\text{Pc})(\text{CN})_2]^-$  is the  $\pi$ -orbital of the  $\text{Pc}$ -ring having  $A_{1u}$  symmetry (8, 9). This orbital forms a conduction band. Degenerate  $E_g$  orbitals are the second HOMOs of  $[M(\text{Pc})(\text{CN})_2]^-$ . These

<sup>1</sup>To whom correspondence should be addressed. Fax: +81-471-36-3236. E-mail: tajima@issp.u-tokyo.ac.jp.

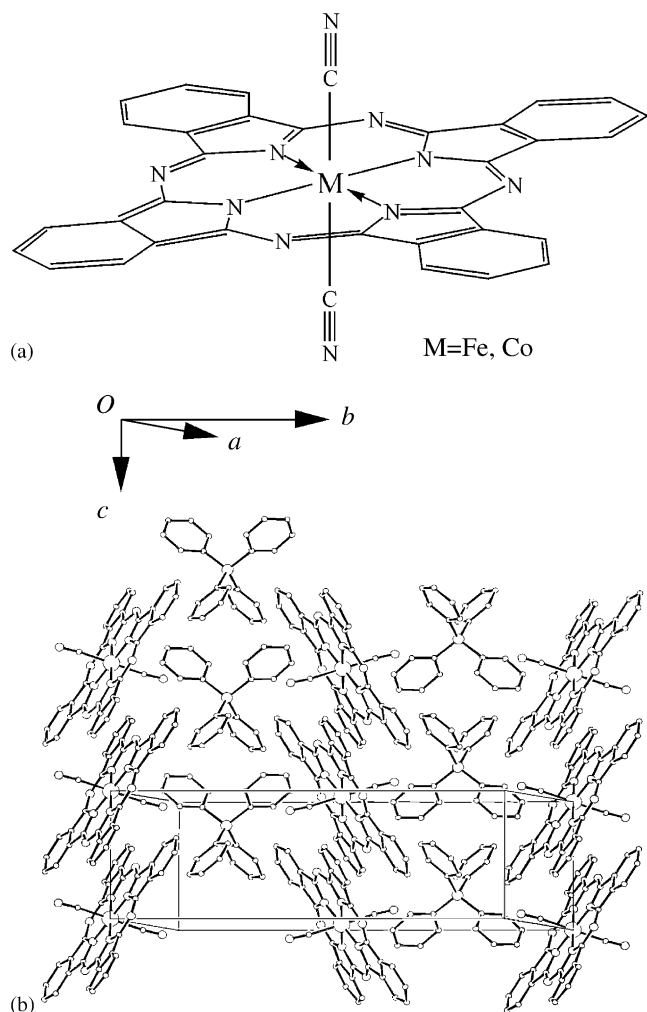


**FIG. 1.** (a) Molecular structure of  $[M(\text{Pc})(\text{CN})_2]^-$  ( $M=\text{Fe}, \text{Co}$ ); (b) crystal structure of  $\text{TPP}[\text{Fe}(\text{Pc})(\text{CN})_2]_2$ . Note that the  $[M(\text{Pc})(\text{CN})_2]^{0.5-}$  units stack along the  $c$ -axis.

orbitals are essentially  $d_{xz}$  and  $d_{yz}$  of the central metal and are potential sources of the local magnetic moments. The  $E_g$  orbitals are completely filled in  $[\text{Co}(\text{Pc})(\text{CN})_2]^-$ , while they are partially filled in  $[\text{Fe}(\text{Pc})(\text{CN})_2]^-$ . Therefore, the  $\pi$ - $d$  interaction is expected in  $[\text{Fe}(\text{Pc})(\text{CN})_2]^-$ , but not in  $[\text{Co}(\text{Pc})(\text{CN})_2]^-$ .

### EXPERIMENTAL

The sample crystals were prepared by an electrocrystallization technique described elsewhere (6–9). We made the gold pads on the  $ac$ -plane of the sample by gold vapor deposition, attached the four gold wires to these pads, and fixed them by gold and carbon paint. The dc four-probe resistance was measured with the current along the  $c$ -axis. In the high-resistance measurements, we applied the constant voltage in series to the sample and the standard

resistance, and measured the sample current and the sample voltage.

### RESULTS

#### $\text{TPP}[\text{Fe}(\text{Pc})(\text{CN})_2]_2$

Fig. 1b shows the crystal structure of  $\text{TPP}[\text{Fe}(\text{Pc})(\text{CN})_2]_2$ . The  $[\text{Fe}(\text{Pc})(\text{CN})_2]$  units form a one-dimensional column elongated along the  $c$ -axis. The crystal parameters are tetragonal,  $P4_2/n$ ,  $a = 21.722 \text{ \AA}$ ,  $c = 7.448 \text{ \AA}$  (8). The infrared optical conductivity spectra of this compound are similar to those of  $\text{TPP}[\text{Co}(\text{Pc})(\text{CN})_2]_2$  (8). This indicates that the electronic structures of  $\text{TPP}[\text{Fe}(\text{Pc})(\text{CN})_2]_2$  and  $\text{TPP}[\text{Co}(\text{Pc})(\text{CN})_2]_2$  are essentially the same at least as for the  $\pi$ -conduction band. The electrical resistivity of  $\text{TPP}[\text{Fe}(\text{Pc})(\text{CN})_2]_2$  drastically increases on lowering the temperature ( $R_{20 \text{ K}}/R_{300 \text{ K}} \sim 2.5 \times 10^5$ ;  $E_a = 16 \text{ meV}$  at  $T = 55 \text{ K}$ ;  $E_a = 30 \text{ meV}$  at  $T = 30 \text{ K}$ ) (8). On the contrary, the resistivity increase on lowering the temperature is not so large in  $\text{TPP}[\text{Co}(\text{Pc})(\text{CN})_2]_2$  ( $R_{20 \text{ K}}/R_{300 \text{ K}} \sim 9$ ;  $E_a = 2.7 \text{ meV}$  at  $T \leq 80 \text{ K}$ ) (7). This difference suggests that the additional scattering mechanism associated with the  $\pi$ - $d$  interaction plays an important role in the electrical conduction in  $\text{TPP}[\text{Fe}(\text{Pc})(\text{CN})_2]_2$ .  $\text{TPP}[\text{Fe}(\text{Pc})(\text{CN})_2]_2$  exhibits anisotropic Curie–Weiss behavior down to 20 K (10) and spontaneous magnetization below 6 K due to weak ferromagnetism (9), while  $\text{TPP}[\text{Co}(\text{Pc})(\text{CN})_2]_2$  exhibits Pauli paramagnetic temperature dependence of the susceptibility (8).

Figure 2 shows the temperature dependence of the resistivity for  $\text{TPP}[\text{Fe}(\text{Pc})(\text{CN})_2]_2$  under magnetic fields of

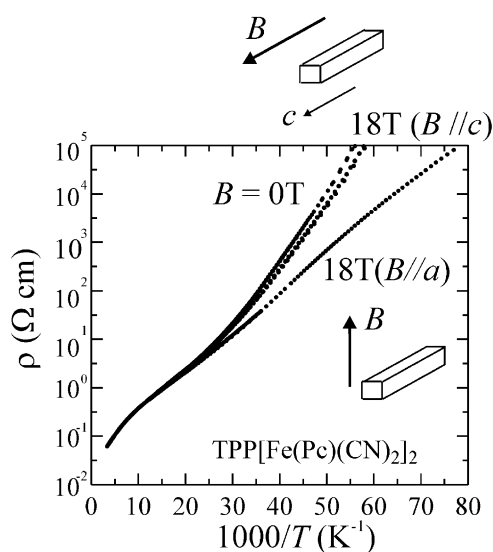


**FIG. 2.** Temperature dependence of the electrical resistivity under the magnetic field applied parallel to the  $c$ - or  $a$ -axis.

18 and 0 T (10). As can be seen from the figure, the resistivity drastically decreases under the applied magnetic field. Noteworthy is the fact that the negative magnetoresistance in this salt is highly anisotropic for the magnetic-field orientation. This field-orientation dependence is consistent with that in the magnetic susceptibility. The Curie constant for the field of  $B \parallel a$  is more than 5–10 times larger than that for the field of  $B \parallel c$ . We considered that this anisotropic behavior (magnetoresistance and magnetic susceptibility) comes from the  $g$ -tensor anisotropy in the  $[\text{Fe}(\text{Pc})(\text{CN})_2]$  unit. In order to make certain of this point, we measured the ESR spectra of  $\{(\text{C}_6\text{H}_5)_3\text{P}\}_2\text{N}[\text{Fe}(\text{Pc})(\text{CN})_2]$  (note: no ESR signal was observed for  $\text{TPP}[\text{Fe}(\text{Pc})(\text{CN})_2]_2$ ), and determined the  $g$ -tensor of  $[\text{Fe}(\text{Pc})(\text{CN})_2]^-$  to be  $g_1 = 3.6$ ,  $g_2 = 1.1$  and  $g_3 = 0.5$  (11). Here,  $g_1$  denotes the  $g$ -factor for the static magnetic field approximately perpendicular to the Pc-ring, and  $g_2$  and  $g_3$  denote the two  $g$ -factors for the field approximately parallel to the Pc-ring. The deviation of the  $g$ -tensor principal axes from the principal axes of the molecular unit and the difference between  $g_2$  and  $g_3$  indicate that magnetic interaction between  $[\text{Fe}(\text{Pc})(\text{CN})_2]$  units is not negligible even in  $\{(\text{C}_6\text{H}_5)_3\text{P}\}_2\text{N}[\text{Fe}(\text{Pc})(\text{CN})_2]$ . In any case, this experimental result revealed that the  $g$ -factor for the field perpendicular to the Pc-ring is much larger than that for the field parallel to the Pc-ring. This large anisotropy in the  $g$ -tensor can be semi-quantitatively explained by the incomplete quenching of the orbital angular momentum under the four-fold symmetry of the ligand field. The larger  $g$ -factor effectively increases the strength of the magnetic field as for the Zeeman energy. Since the orientation component perpendicular to the Pc-ring is larger in the  $a$ -axis than in the  $c$ -axis, as shown in Table 1, the larger negative magnetoresistance and the larger Curie constant is expected for the field orientation parallel to the  $a$ -axis. This expectation is consistent with the observed anisotropy in the magnetoresistance and in the magnetic susceptibility. In other words, the anisotropy in the magnetoresistance reflects the molecular geometry of

the  $[\text{Fe}(\text{Pc})(\text{CN})_2]$  unit in the crystal through its anisotropic  $g$ -tensor.

### $\text{TPP}[\text{Co}(\text{Pc})(\text{CN})_2]_2$

As mentioned above, the crystal structure of this salt is similar to  $\text{TPP}[\text{Fe}(\text{Pc})(\text{CN})_2]_2$ . The crystal parameters are tetragonal,  $P4_2/n$ ,  $a = 21.676 \text{ \AA}$ ,  $c = 7.474 \text{ \AA}$  (7). Figure 3 shows the temperature dependence of the electrical resistivity under the magnetic field. In contrast with  $\text{TPP}[\text{Fe}(\text{Pc})(\text{CN})_2]_2$ , this salt exhibits positive magnetoresistance. One may consider that this positive magnetoresistance is due to the orbital effects, which is usually observed in the magnetoresistance in molecular conductors. However, field-orientation dependence of the magnetoresistance is not so large in this salt in spite of the quasi-one-dimensional character of the electronic structure. This

**TABLE 1**  
The Relation between the Anisotropy in Negative Magnetoresistance (Positive Magnetoconductivity) and the Molecular Orientation of the  $[\text{Fe}(\text{Pc})(\text{CN})_2]$  Unit in the  $\text{TPP}[\text{Fe}(\text{Pc})(\text{CN})_2]_2$  Crystal

$\text{TPP}[\text{Fe}(\text{Pc})(\text{CN})_2]_2$	$B \parallel a$ (18 T)	$B \parallel c$ (18 T)
$-\Delta R/R$ ( $\Delta\sigma/\sigma$ )		
30 K	0.582 (1.39)	0.212 (0.27)
20 K	0.941 (16.0)	0.522 (1.09)
Axial vector of the $\text{Fe}(\text{Pc})(\text{CN})_2$ unit ( $\vec{l} \parallel \text{NC}-\text{Fe}-\text{CN}$ bond)		
Molecule 1	$l_a$ : 0.828	$l_c$ : 0.270
Molecule 2	$l_a$ : 0.492	$l_c$ : 0.270

Note.  $l_a$  ( $l_c$ ): the  $a$ -axis ( $c$ -axis) component of the elementary vector perpendicular to the Pc-ring.

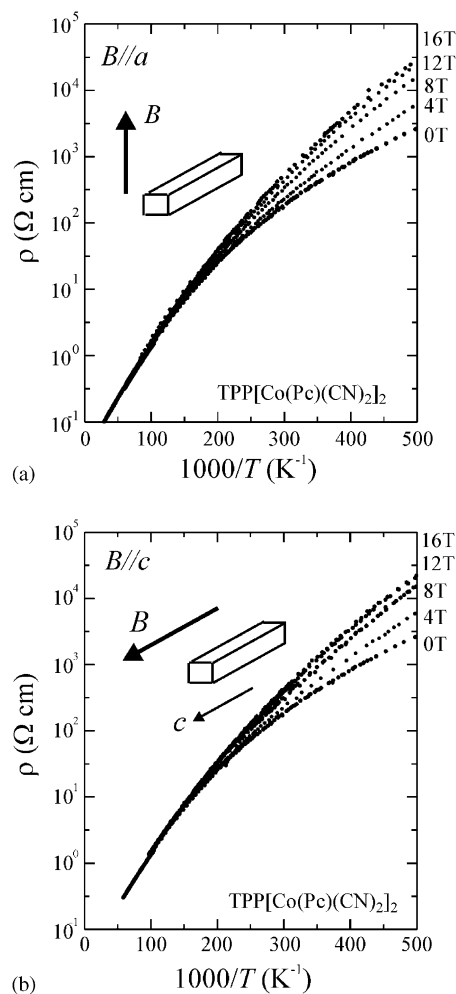


**FIG. 3.** Temperature dependence of the electrical resistivity under magnetic fields of 16, 12, 8, 4, 0 T applied parallel to the  $a$ -axis (a) and to the  $c$ -axis (b).

behavior is not well understood by the classical model of the magnetoresistance based on the Boltzmann equation theory.

### $TPP[Fe_{0.30}Co_{0.70}(Pc)(CN)_2]_2$

The crystal structures of  $TPP[Fe(Pc)(CN)_2]_2$  and  $TPP[Co(Pc)(CN)_2]_2$  are similar to each other, and these two salts form alloys. Figure 4a shows the temperature dependence of the electrical resistivity of the alloy. The molar ratio of Fe and Co contents was determined by SEM-EDS analysis. The crystal parameters are tetragonal,  $P4_2/n$ ,  $a = 21.67 \text{ \AA}$ ,  $c = 7.45 \text{ \AA}$ . As can be seen from the figure, the alloy exhibits intermediate behavior between  $TPP[Fe(Pc)(CN)_2]_2$  and  $TPP[Co(Pc)(CN)_2]_2$  ( $E_a = 12 \text{ meV}$  at  $T = 14 \text{ K}$ ;  $E_a = 9.8 \text{ meV}$  at  $T = 30 \text{ K}$ ). Figure 4b shows the electrical resistivity of  $TPP[Fe_{0.30}Co_{0.70}(Pc)(CN)_2]_2$  under the magnetic field. The alloy exhibits aniso-

tropic magnetoresistance similarly to  $TPP[Fe(Pc)(CN)_2]_2$ . However, the negative magnetoresistance is not only weakened but also less anisotropic for the field orientation.

### Comparison with the Negative Magnetoresistance in $(Cu_xNi_{1-x}Pc)(I_3)_{1/3}$

In the following, we compare the magnetoresistance data of  $TPP[M(Pc)(CN)_2]_2$  ( $M = Fe, Co, Fe_{0.30}Co_{0.70}$ ) with those of  $(Cu_xNi_{1-x}Pc)(I_3)_{1/3}$  obtained by the microwave technique. According to Quirion *et al.* (5), only the negative magnetoresistance is observed in  $(Cu_xNi_{1-x}Pc)(I_3)_{1/3}$  ( $x \leq 0.5$ ), both positive and negative magnetoresistances in  $(Cu_xNi_{1-x}Pc)(I_3)_{1/3}$  ( $0.75 \geq x \geq 0.65$ ), and only the positive magnetoresistance is observed in  $(CuPc)(I_3)_{1/3}$ . The negative magnetoresistance becomes largest at  $x = 0.25$ .  $(CuPc)(I_3)_{1/3}$  has local magnetic moments originating from  $Cu^{II}$ , while  $(NiPc)(I_3)_{1/3}$  does not have any local magnetic moments. As for the sign of the magnetoresistance versus the concentration of the local magnetic moment, the tendency for  $(Cu_xNi_{1-x}Pc)(I_3)_{1/3}$  is seemingly the reversal of the tendency for  $TPP[M(Pc)(CN)_2]_2$ . Quirion *et al.* argued that the absence of the negative magnetoresistance in  $(CuPc)(I_3)_{1/3}$  is due to the freezing of the spin degrees of the freedom by the very strong magnetic coupling between the local magnetic moments, and that the negative magnetoresistance in  $(NiPc)(I_3)_{1/3}$  is due to the magnetic impurities. If we follow this interpretation, the seemingly reversal tendency can be explained by the assumption that spin degrees of the freedom do not completely vanish in  $TPP[Fe(Pc)(CN)_2]_2$ .

What does this mean? One may consider that the magnetic coupling between the local moments is weaker in  $TPP[Fe(Pc)(CN)_2]_2$  than in  $(CuPc)(I_3)_{1/3}$ . However, the Weiss temperature, which is a measure of magnetic coupling, is more than three times larger in  $TPP[Fe(Pc)(CN)_2]_2$  than in  $(CuPc)(I_3)_{1/3}$ . [ $\Theta = -4 \text{ K}$  in  $(CuPc)(I_3)_{1/3}$  (12);  $\Theta = -13.7 \text{ K}$  in  $TPP[Fe(Pc)(CN)_2]_2$  (10)]. This is against the consideration above. At the present stage, the most plausible answer to this question is to consider an additional weak interaction between local magnetic moments [such as Dzyaloshinski–Moriya interaction (13)] other than the strong antiferromagnetic interaction. Under the influence of such a weak interaction, the local magnetic moments fall into a state different from the genuine antiferromagnetic state (typically the weak-ferromagnetic state). Before falling into such a magnetic state, there should be a magnetic fluctuation associated with the phase transition. Since this magnetic fluctuation arises from the weak interaction, the applied magnetic field effectively works for orienting the magnetic moments. In other words, the giant negative magnetoresistance in

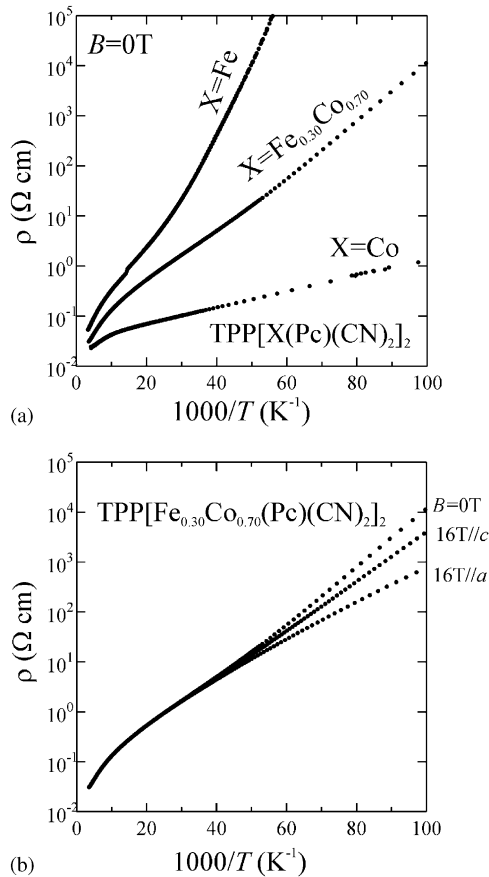


**FIG. 4.** (a) Temperature dependence of the electrical resistivity of  $TPP[Fe(Pc)(CN)_2]_2$ ,  $TPP[Fe_{0.3}Co_{0.7}(Pc)(CN)_2]_2$ , and  $TPP[Co(Pc)(CN)_2]_2$ ; (b) temperature dependence of the electrical resistivity under the magnetic field applied parallel to the  $a$ - or  $c$ -axis.

TPP[Fe(Pc)(CN)<sub>2</sub>] may be a precursor effect of some magnetic transition associated with the weak interaction. In this context, the appearance of the spontaneous magnetization [TPP[Fe(Pc)(CN)<sub>2</sub>];  $T < 6$  K] which manifests a magnetic transition into a weak-ferromagnetic state is noteworthy (9).

If the above-mentioned arguments are true, we have not yet observed giant negative magnetoresistance associated with the antiferromagnetic interaction itself. In order to observe this, it may be necessary to apply higher magnetic field or to weaken the antiferromagnetic interaction.

#### ACKNOWLEDGMENTS

This work was partly supported by a Grant-in-Aid for Scientific Research, from the Ministry of Education, Science and Culture, Japanese Government. Part of the work was performed using facilities in Analysis Laboratory, the Material Design and Characterization Laboratory, ISSP.

#### REFERENCES

1. S. Uji, H. Shinagawa, T. Terashima, T. Yakabe, Y. Terai, M. Tokumoto, A. Kobayashi, H. Tanaka, and H. Kobayashi, *Nature* **410**, 908–910 (2001); L. Brossard, R. Clerac, C. Coulon, M. Tokumoto, T. Ziman, D. K. Petrov, V. N. Laukin, M. J. Naughton, A. Audouard, F. Goze, A. Kobayashi, H. Kobayashi, and P. Cassoux, *Eur. Phys. J. B* **1**, 439–452 (1998); H. Kobayashi, H. Tomita, T. Naito, A. Kobayashi, F. Sakai, T. Watanabe, and P. Cassoux, *J. Am. Chem. Soc.* **118**, 368–377 (1996).
2. C. S. Schramm, R. P. Scaringe, D. R. Stojakovic, B. M. Hoffman, J. A. Ibers, and T. J. Marks, *J. Am. Chem. Soc.* **102**, 6702–6713 (1980); J. Martinsen, S. M. Palmer, J. Tanaka, R. Greene, and B. M. Hoffman, *Phys. Rev. B* **30**, 6269–6276 (1984).
3. T. Inabe, T. J. Marks, R. L. Burton, J. W. Lyding, W. J. McCarthy, C. R. Kannewurf, G. M. Reisner, and F. H. Herbstein, *Solid State Commun.* **54**, 501–503 (1985); T. Inabe, S. Nakamura, W. Liang, T. J. Marks, R. L. Burton, C. R. Kannewurf, and K. Imaeda, *J. Am. Chem. Soc.* **107**, 7224–7226 (1985).
4. K. Yakushi, M. Sakuda, H. Kuroda, A. Kawamoto, and J. Tanaka, *Chem. Lett.* **1986**, 1161–1164 (1986).
5. G. Quirion, M. Poirier, K. K. Liou, and B. M. Hoffman, *Phys. Rev. B* **43**, 860–864 (1991).
6. M. Matsuda, T. Naito, T. Inabe, N. Hanasaki, H. Tajima, *J. Mater. Chem.* **11**, 2493–2497 (2001).
7. H. Hasegawa, T. Naito, T. Inabe, T. Akutagawa, and T. Nakamura, *J. Mater. Chem.* **8**, 1567–1570 (1998).
8. M. Matsuda, T. Naito, T. Inabe, N. Hanasaki, H. Tajima, T. Otsuka, K. Awaga, B. Narymbetov, and H. Kobayashi, *J. Mater. Chem.* **10**, 631–636 (2000).
9. M. Matsuda, Thesis, The Graduate School of Science, Hokkaido University, March 2001.
10. N. Hanasaki, H. Tajima, M. Matsuda, T. Naito, and T. Inabe, *Phys. Rev. B* **62**, 5839–5842 (2000).
11. N. Hanasaki, M. Matsuda, H. Tajima, T. Naito, T. Inabe, *Synth. Met.*, in press.
12. M. Y. Ogawa, S. M. Palmer, K. Liou, G. Quirion, J. A. Thompson, M. Poirier, and B. M. Hoffman, *Phys. Rev. B* **39**, 10682–10692 (1989).
13. I. Dzyaloshinsky, *J. Phys. Chem. Solids* **4**, 241 (1958); T. Moriya, *Phys. Rev.* **120**, 91–98 (1960).